Uranium Behavior in Jurassic Fish Coprolites: Combined Microbeam Synchrotron X-Ray Fluorescence, Diffraction, and XANES Analysis

A. Lanzirotti[1], M. Becker[2], G.N. Hanson[2], and S.R. Sutton[1]
[1]University of Chicago, [2]State University of New York-Stony Brook

Worldwide, the anoxic, organic-rich sediments collectively referred to as "black shales" are know to be an important sink for oceanic uranium. There have been estimates that suggest that as much as 20% of the annual fluvial input of U into the world's oceans may be bound in such organic-rich strata [1]. Adsorption of U onto organic matter has been suggested as an essential preconcentration step in the formation of many sedimentary ore deposits. However, the bio-geochemical processes by which U is incorporated into these sediments are still not clearly understood. The redox conditions and kinetics at the sediment-water interface, the amount of organic material present, fluid-mineral and mineral-mineral reactions are all known to play important roles in how U is incorporated [1,2,3].

Here we present microbeam synchrotron x-ray fluorescence, diffraction, and XANES analyses from beamline X26A at the NSLS on a single thin-section of a Jurassic fish coprolite from a black-shale horizon in central Connecticut (ca. 198 million years old). Coprolites are fossilized fecal material and, as such, clearly contained organic material at one time. These coprolites, now preserved as phosphatic material, are unusual in that they have very high levels of uranium, often in excess of 600 ppm. This provides an opportunity to evaluate the mineral and organic interactions that have resulted in the partitioning of U into these coprolites. This study also demonstrates the unique microbeam capabilities of the X26A beamline for near simultaneous evaluation of major and trace element compositions using synchrotron x-ray fluorescence (XRF), elemental speciation using fluorescence mode x-ray absorption near-edge spectroscopy (XANES), and mineralogy using micro x-ray diffraction (XRD) of geologic and environmental samples at spatial resolutions of ~10μm.

Geology and Mineralogy:

The Shuttle Meadow Formation was deposited as rift-basin sediments and is the lowermost Jurassic sedimentary unit of the Hartford Basin in southern Connecticut. Although siliciclastic alluvial sediments dominate the formation, it's lowermost section contains a single black shale horizon that is believed to represent the deposition of sediment in an offshore lake environment. This black shale contains abundant, fully articulated fish fossils (genus *Semionotus, Redfieldius, Diplurus*) and their associated coprolites. Now preserved as phosphatic minerals, the original organic material in these coprolites provided a nucleation site for HPO_4^-, resulting in the precipitation of phosphate. During early diagenesis, phosphatization begins before the complete decay of organic material and additional HPO_4^- may be introduced by the decay of fish debris (fish teeth and bones composed of hydroxyapatite) contained within the coprolite.

Figure 1 shows two photomicrographs of thin-sections that were made through the coprolite that we discuss in this study. In this discussion, we will focus on this one particular sample because of its well-preserved optical zoning. Figure 1a shows the coprolite section that was analyzed at X26A. The coprolite is the dark black, layered material in the image and is surrounded by matrix minerals of the host shale (the fine, gray layers on the margin). The labeled points on the image show where the discussed analyses were taken (see figure caption). Figure 1b is a photomicrograph of a second section through this same coprolite. This section was heated at 450°C for 4 days. As a result of this heating the coprolite has turned from opaque black to light brown, accentuating many of the internal structural details that were not visible before. The change in color and opacity are likely the result of pyrolization of organic matter in the section, indirectly showing that these coprolites still contain organics. The layering in the coprolite most likely reflects variability in either composition (mineralogic or organic) or grain size, or both.

Analyses were conducted on 300 μm thick polished sections of coprolite mounted on glass with epoxy. The incident beam was tuned to the U L_{III} binding energy using our Si(111) channel-cut monochromator. This 350 μm collimated monochromatic beam is then focused to 10 μm in diameter using our system of Rh coated Kirckpatrick-Baez mirrors [4]. XRF compositional data and fluorescence mode XANES were collected using a Canberra SL30165 Si(Li) detector. Elemental abundances were calculated using a modified version of NRLXRF [5], designed for "standard-less" analysis of XRF spectra obtained with monochromatic radiation.

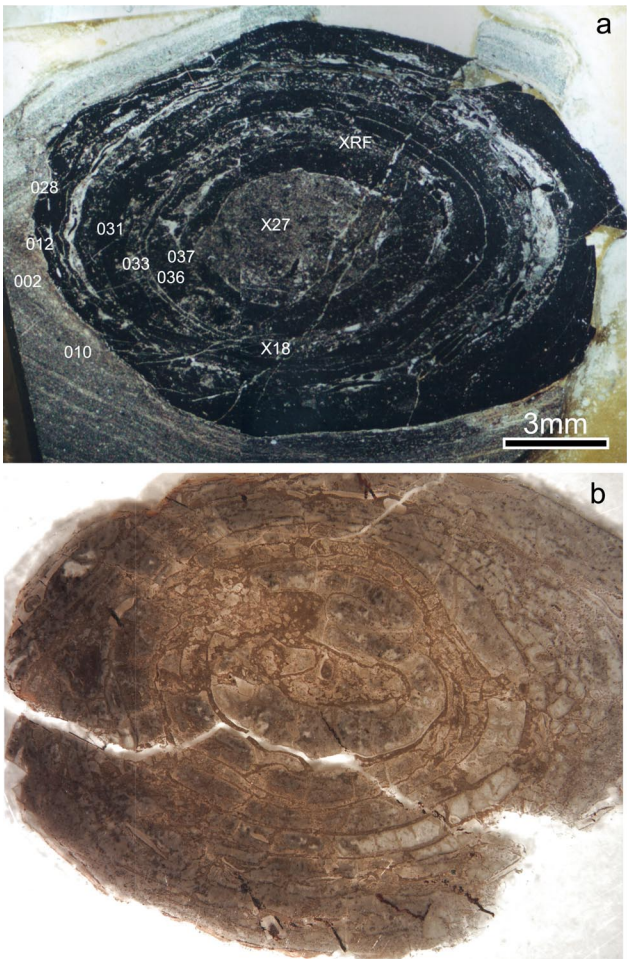

Figure 1: a) Photomicrograph of the Jurassic fish coprolite (fossilized fecal material) analyzed in this study. The sample numbers "002, 010, 012, 028, 031, 033, 036, and 037" are synchrotron microbeam XRD analyses discussed in the text. Sample numbers "X18, and X27" are XANES analyses discussed in the text. The spot labeled "XRF" is the XRF spectra shown as an inset in Figure 4. b) Photomicrograph of a separate section of this coprolite that was heated at 450°C for four days.

This standard-less approach uses an internal reference element, in this case the Ca concentration in the hydroxyapatite that composes the coprolite (fixed by stoichiometry), and computes relative sensitivities using the prediction capabilities of NRLXRF. U XANES data were collected in fluorescence mode by scanning the monochromator through the U L_{III} binding energy. XANES energy calibrations are based on analysis of UO_2 and UO_3 standards and are plotted relative to the U L_{III} absorption edge of 17,166 eV, normalized to photon flux monitored by an upstream ion chamber. Every third XANES spectrum collected was a re-analysis of the UO_2 standard to monitor for energy drifts due primarily to monochromator heating with time. Any such drifts were then corrected. Microbeam XRD data were collected using a Brucker SMART CCD system in reflection mode geometry. The wavelength of the incident beam during the diffraction analyses was kept at 0.7976 Å. Because of the small spot size of the incident beam relative to the grain size of the minerals in the section, the intensity of diffraction peaks can be strongly affected by grain size and the preferred orientation of minerals in thin section. The more coarsely crystalline the material is, the greater the divergence from a typical powder pattern.

Microbeam XRD Results:

Quantitative identification of mineralogy in shales is often difficult because of the cryptocrystalline character of the minerals. Accurate determinations by optical petrography are often impossible and compositional analysis by electron beam microanalysis usually only indirectly identifies the mineral. Synchrotron microbeam XRD provides a unique method by which to quantitatively identify such minerals in-situ and provides conclusive results when coupled with simultaneous XRF measurements. Figure 2 shows a series of XRD patterns collected on the coprolite section shown in Figure 1a. The inset images show representative CCD diffraction patterns from each group of analyses. The figure on the left, labeled "Matrix," shows four diffraction patterns collected on matrix phases at spots 002 and 010, well within the surrounding matrix, and 012 and 028, in the matrix but adjacent to the coprolite boundary. Note that although the patterns are "spotty," they are still good powder patterns, consistent with an average grain size much smaller than the diameter of the incident beam (~10 µm). Also shown are diffraction patterns for quartz (red) and dolomite (blue). The XRD data are consistent with the mineralogy of the matrix being dominated by these two phases. This is a bit unusual for black-shales, which typically have higher clay contents and less carbonate. The plot on the right, labeled "Coprolite," shows four XRD patterns collected within the coprolite itself. Analyses 031 and 036 are within the darker bands and analyses 033 and 037 are in the lighter colored bands. The majority of the diffraction peaks can be accounted for by the minerals hydroxyapatite (orange) and dolomite (blue). Note that there is little difference between the diffraction patterns from dark and light colored bands, suggesting little difference in bulk mineralogy between these zones. No distinct U bearing minerals such as uraninites are identifiable. It is important to note, however, that in our present mode of operation differences in organic content would not be detected.

Microbeam XRF Results:

Figure 3 shows a set of four XRF compositional maps of the coprolite shown in Figure 1a. A typical XRF

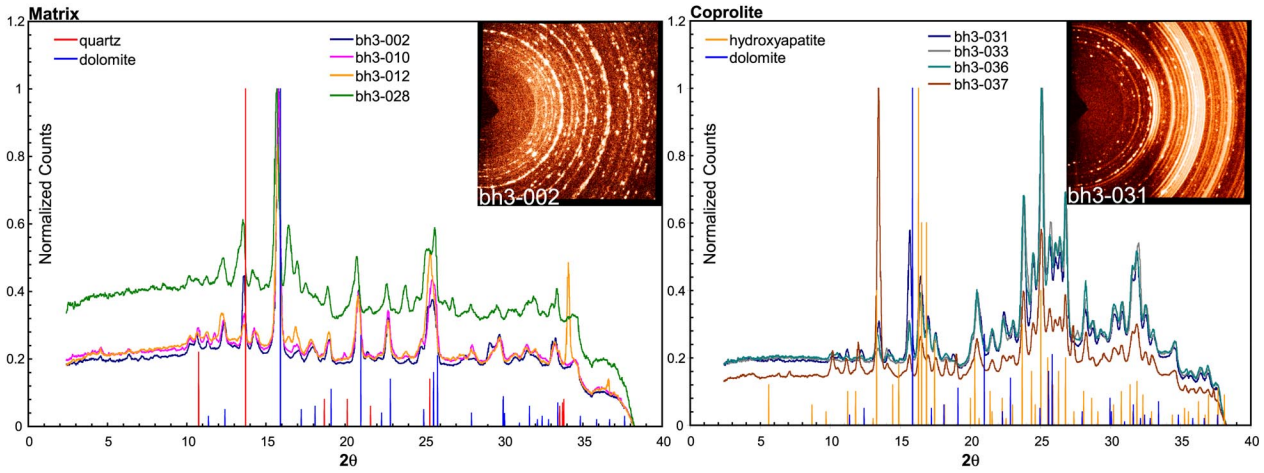

Figure 2: Intensity vs. 2-theta microbeam x-ray diffraction patterns for selected points in the matrix (left) and coprolite (right) shown in Figure 1a. Also superimposed are diffraction patterns for dolomite (blue), quartz (red), and hydroxyapatite (orange). The inset figures show representative Brucker CCD diffractometer patterns for each group of analyses, 002 for the matrix and 031 for the coprolite.

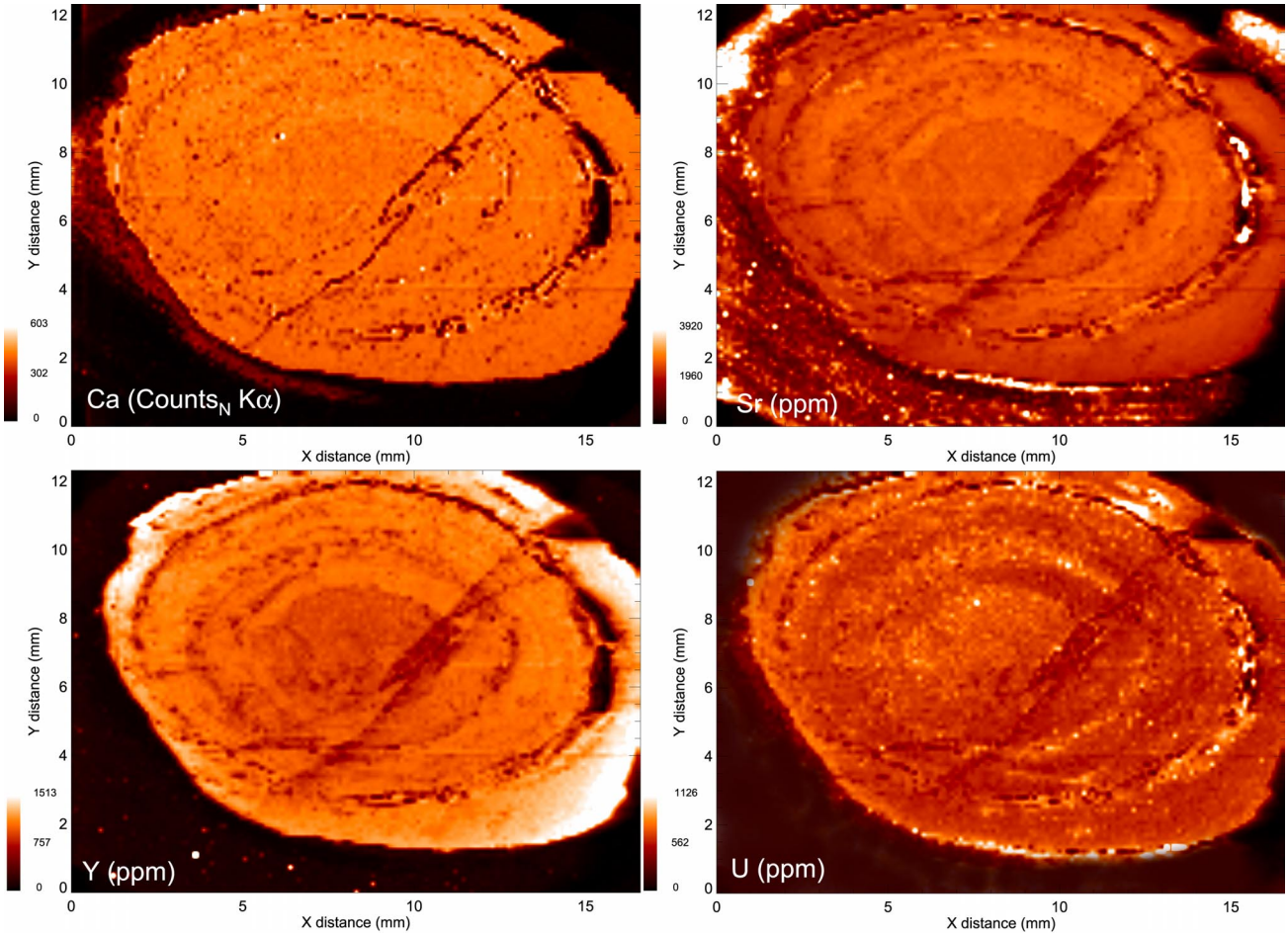

Figure 3: Synchrotron microbeam XRF compositional maps of the coprolite shown in Figure 1a. Ca is shown in normalized counts for the Ca Kα fluorescence peak, Sr, Y, and U are in ppm.

energy dispersive spectrum is shown as an inset in Figure 4. The map for Ca is shown in normalized counts on the Ca Ka peak while the other three maps are in ppm. The Ca map shows that although the Ca fluorescence in the coprolite is generally uniform, there are some variations that correlate with the optical variations seen in thin section. The XRD results suggest this is not a result of mineralogic variability between bands. It is possible, however, that such variations could be accounted for by variability (type or abundance) in the organic matter between bands. Sr^{2+} and Y^{3+} both commonly substitute for Ca in the apatite structure, since they have similar ionic radii and charge, although Y incorporation usually requires coupled substitution of ionic complexes, such as SiO_4 for PO_4, to maintain charge balance. In the compositional mapping, there is a clear correlation of Sr and Y abundance with Ca and with the optical zoning in the coprolite. The U XRF compositional map shows that U abundance throughout the coprolite is high (~600 ppm average) relative to the matrix and that the U displays compositional zoning that correlates with the optical zoning in the hydroxyapatite. U is also known to be a common trace element in apatite and is often used for U^{238} fission track dating of geologic materials. How U is incorporated into the apatite structure is still debated (and dependant on it's oxidation state), but in most models U (most likely as 4+, ionic radius of 0.97 Å) substitutes for Ca 2+ (ionic radius of 0.99 Å) in its 7- and 9-fold coordinated sites, with some coupled substitution to account for charge balance. Thus, it should mimic the behavior of Y. What the XRF analyses demonstrate, however, is that the U abundance in this coprolite (~400-1000 ppm) is inversely correlated with Ca, Sr, and Y.

XANES Results:

Figure 4 shows two representative XANES spectra collected from the coprolite. Although there is some variability in edge position, particularly for analyses within 100 µm of the coprolite edge, the XANES spec-

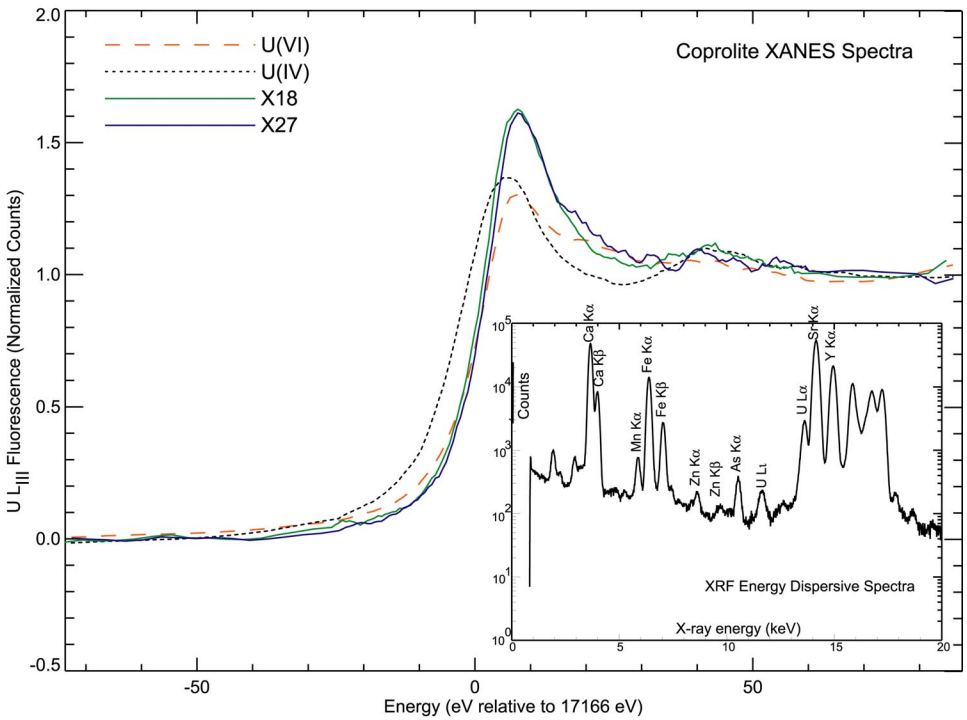

Figure 4: U L_{III} XANES spectra for the UO_2 and UO_3 standards and two selected points in the coprolite (X18, and X27 in Figure 1a). Spectra are normalized to their respective edge steps.

tra throughout most of the coprolite is very similar to the two spectra shown here. Analysis X18 is midway to the center of the coprolite in a high U band and analysis X27 is from the U rich center of the coprolite. These analyses are superimposed with XANES spectra of our UO_2 and UO_3 standards. Although structure and matrix effects may have the potential to produce an edge shift, it is clear that relative to the UO_2 standard, the relative XANES edge energies of these analyses are shifted towards higher energy. Additionally, these spectra have a small post-edge multiple resonance peak similar to the "shoulder" typically observed in U(VI) XANES spectra [2]. It is thus likely that much of the U in this particular sample is oxidized and dominated by U(VI).

Although it is no surprise that a black-shale such as that preserved in the Shuttle Meadow formation or the phosphates contained within it are high in U, the microbeam analyses at X26A provide interesting insights into the geochemistry of U incorporation in such sediments. It is clear from the XRF energy dispersive analyses that the coprolites themselves are the dominant U bearing material in these sections. The microbeam XRD data show that the primary mineralogic difference between matrix and coprolite is the presence of hydroxyapatite. It would seem logical to conclude that early phosphotization of the coprolite provided a site for U incorporation into the apatite structure. However, the XRF compositional mapping shows an inverse correlation between U (which should substitute for Ca) and other trace element constituents such as Sr and Y that are known to substitute for Ca in apatite. It is likely that the high U abundances may reflect complexation of U with the organic matter in the coprolite close to the time of diagenesis of the sediment under anoxic conditions. Bacterial sulphate reduction can then release dissolved HCO_3^-, HPO_4^-, and NH_4^+ and provide a nucleation site for HPO_4^-, resulting in the precipitation of phosphate. In such a scenario the U abundance is controlled primarily by the abundance of organic C, rather than the abundance of phosphate. What is then difficult to explain is why the XANES analyses suggest the presence of oxidized U in these samples. Black-shales are known to form beneath oxygen depleted bottom waters and to be rich in organic C, which could be assumed to favor chemical and/or biological reduction of U during sedimentation. In this case, later oxidation of the U is needed to explain the speciation we observe in these coprolites today. Such reactions could be related to later lithification of the sediment. However, some studies have shown that in some sediments deposited under reducing conditions often the first U solids to precipitate are predominantly U(VI) [2]. Duff et al. were able to demonstrate that even under low Eh conditions reaction kinetics often still favor the precipitation of U(VI) solids. Although at this time these questions cannot be quantitatively evaluated, future EXAFS and FTIR analyses may provide better insights into how U is bound in these unique samples. But the observation that much of the uranium may potentially be bound to organic matter is consistent with other recent studies of black-shales that have found that despite the presence of potential U-rich diagenetic phases such as apatite and monazite, most of the U is associated with non-extractable diagenetic components such as organics [6].

Aknowledgements:

This research was funded by grant DOEFG0292ER14244 to S. Sutton and DERO294ER14449 to G. Hanson and W. Meyers. The microdiffraction studies are a collaborative effort between A. Lanzirotti and John Parise (SUNY Stony Brook, Geosciences) to promote advances in environmental microdiffraction studies at X26A. The installation of the Bruker CCD facility at the NSLS was supported by the NSF through grant EAR-9724501/Stony Brook to John Parise.

References:

[1] C.E. Barnes and J.K. Cochran, "Geochemistry of Uranium in Black Sea Sediments," Deep-Sea Research, **38**, p. S1237-S1254, 1991.

[2] M.C. Duff et al., "The chemistry of Uranium in Evaporation Pond Sediment in the San Joaquin Valley, California, USA, using X-ray Fluorescence and XANES Techniques," Geochimica et Cosmochimica Acta, **61**, p.73-81, 1997.

[3] D.R. Lovely et al., "Microbial Uranium Reduction," Nature, **350**, p.413-416, 1991.

[4] P. J. Eng, M. Newville, M.L. Rivers, and S.R. Sutton, "Dynamically figured Kirkpatrick Baez micro-focusing optics," in X-Ray Microfocusing: Applications and Technique, I. McNulty, ed., Proceedings SPIE, **3449**, p. 145, 1998.

[5] J.W. Criss, "NRLXRF, A FORTRAN Program for X-Ray Fluorescence Analysis," Naval Research Laboratory, Washinghton, D.C., 1977.

[6] S.M. Lev, S.M. McLennan, AND G.N. Hanson, "Late Diagenetic Redistribution of Uranium and Disturbance of the U-Pb Whole Rock Isotope System in a Black Shale," Journ. Of Sedimentary Research, **70**, 2000.

Evaluating Heterogeneous Reactivity at the Mineral-Water Interface from Sectoral Zoning of REEs, Sr and Y in Fluorite

J. Rakovan[1], S. Bosze[1], and A. Lanzirotti[2]
[1]Miami University, Oxford, OH, [2]University of Chicago-CARS

One of the hallmarks of mineral surface reactivity is its heterogeneous nature. Not only do different minerals behave in strikingly different fashions, but also within the confines of a single mineral's surface, reactivity can vary significantly. A fundamental insight gained from mineral surface studies is that a bulk atomic site within a crystal may have multiple, distinctly different surface representations, the presence of which leads to heterogeneous reactivity at the mineral-water or mineral-melt interface (Reeder and Rakovan 1999). One of the most significant geochemical processes that take place at these interfaces is crystal growth.

During crystal growth, minor or trace amounts of substituent elements may become incorporated in regular atomic sites within the crystal. Because trace elements are sensitive indicators of geologic processes, trace element geochemistry has formed the basis for many studies. Applications include the interpretation of petrogenesis, hydrothermal mineralization, water quality and history, and geochronology. Essential to such studies is knowledge of the partitioning of specific trace elements between different phases in a system. Many complex variables affect the partitioning of trace elements into minerals during crystal growth. Recently, numerous authors have demonstrated the role of surface structure on the partitioning of elements into crystals (Paquette and Reeder, 1995, 1995; Northrup and Reeder 1994; Rakovan and Reeder 1994, 1996; Rakovan et al. 1997; Bosze and Rakovan, 1999; Bosze and Rakovan in prep.). We are continuing our studies of the role of crystal surface structure in heterogeneous reactivity of minerals, specifically addressing differential adsorption and incorporation of trace metals into the mineral fluorite. Here the differential incorporation of REEs, Y and Sr into fluorite is being used as a probe of the structural differences between nonequivalent surface sites.

Fluorite crystals from several important hydrothermal mineral deposits, including the Hansonburg Mining District, Bingham, NM (Taggart et al. 1989) and the Long Lake fluorite deposit, St. Laurence fluorite district, NY (Richards and Robinson 2000), are being studied. Crystals from these deposits exhibit multiple, symmetrically nonequivalent crystal forms (Figure 1a). The concentration and distribution of the trace elements within oriented sections of single crystals are measured by spatially resolved synchrotron X-ray fluorescence microanalysis line and area scans.

Standard X-ray fluorescence experiments at X26A have involved the use of energy dispersive (EDS) detectors. Because of the small separation amongst the numerous L fluorescence lines of the REE series, wavelength-dispersive detection is necessary to resolve and quantify individual REE distributions. The increased energy resolution of WDS, 3 eV to 25 eV (FWHM) for most elements, allows for detection of individual REEs. A Microspec WDX-3PC wavelength-dispersive spectrometer is used with a LiF (200) crystal to analyze the REE $L\alpha_1$ and $L\beta_1$ lines. Data are collected using a white synchrotron beam collimated to an incident size between 8 and 100 µm, depending on the spatial resolution necessary to resolve individual sectors (volumes of the crystal that grew by incorporation of growth units or adatoms onto a specific crystal face). Comparison of the peak to background ratios shows that the effective sensitivity, or the minimum detection limit, of the WDS spectrometer is comparable to that of the EDS for the REEs. Figure 2 compares SXRFMA data collected on the same sample using EDS and WDS. Estimated relative precisions for the elements considered here are approximately 1%.

SXRFMA line and area scans show that Sr, Y, and REE compositional differences exist for coeval portions of symmetrically nonequivalent sectors in the fluorites studied (Figures 1 a and b and 3). Such intracrystalline heterogeneities are known as sectoral zoning (SZ). The relationship of sectors to crystal faces suggests that these heterogeneities formed during crystal growth. Two distinct mechanisms for SZ have been identified; differences in the growth rate of nonequivalent crystal faces, and the presence of distinctly different sites of incorporation (on the nonequivalent crystal faces). The internal morphology (concentric zoning and sector shape) of these samples revealed by cathodoluminescence indicates roughly equivalent growth rates of many of the crystal faces associated with the sector zoning. Hence, growth rate anisotropy is not the cause of SZ in these samples.

It is hypothesized that differences in the surface structure of these different crystal faces on fluorite, specifically the structure of sites of incorporation on different faces, lead to different affinities for the trace elements studies, and hence differential incorporation.

Long Lake fluorites exhibit {100} and {111} crystal faces. Figure 1b,c shows the differential distribution of Gd between |111| and |100| sectors associated with

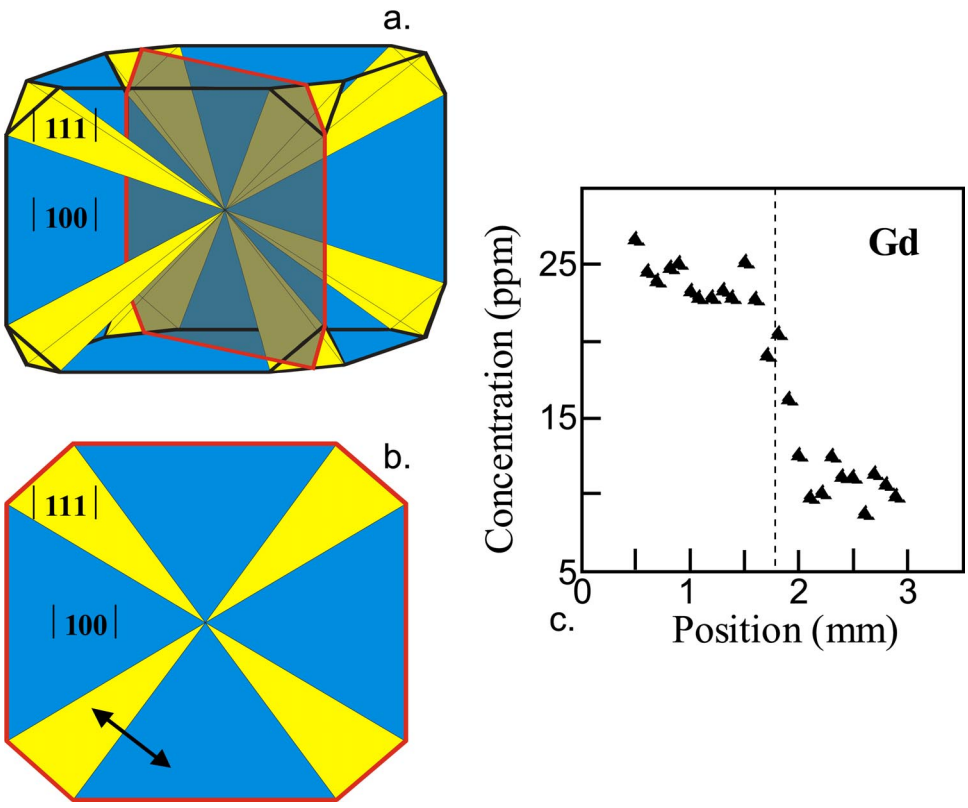

Figure 1. Zoning of Gd between |111| and |100| sectors of fluorite from Long Lake, NY. a) Schematic showing ideal 3D distribution of cube |100| and octahedral |111| sectors (internal morphology) within a cubooctahedral crystal. b) Schematic of thin section taken from crystal in figure 1a. Double arrow indicates the position of an X-ray fluorescence line scan taken between two symmetrically nonequivalent sectors. c) Plot of the concentration of Gd (ppm) along the line scan indicated in b. Figure modified from Bosze and Rakovan (in Rev).

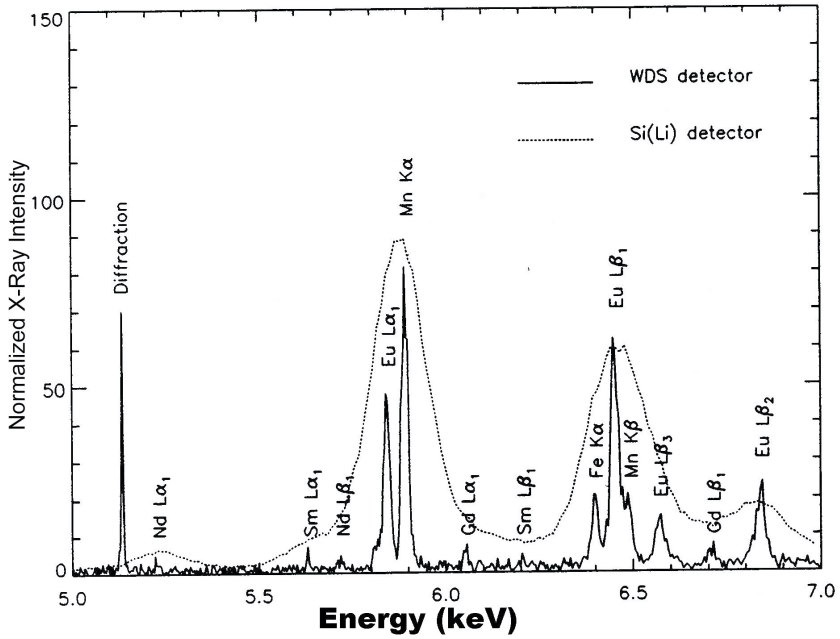

Figure 2. Synchrotron X-ray fluorescence microanalysis (SXRFMA) data collected by EDS (dotted line) and WDS (solid line) from an apatite from Llallagua, Bolivia. Figure modified from Rakovan et al. (2001).

these faces. Fluorites from Bingham, NM are unique in that they exhibit six symmetrically different sectors, with as many as four in any one single crystal. Sectoral zoning of Sr, Y and REEs is found amongst all of the exhibited sectors. Figure 3 shows sectoral zoning of Sr and Y among |111|, |110| and |100| sectors of a Bingham fluorite. Sr is enriched in the |110| sector relative to |111| and |100|, while Y is preferentially incorporated into the |111| sector.

The presence of sectoral zoning in fluorite demonstrates non-equilibrium incorporation and indicates that factors such as growth mechanism and surface structure are important in partitioning. Sectoral zoning not only demonstrates that mechanistic factors play a role in partitioning, but also that partition coefficient, K_d, values for a given mineral-fluid system are not unique. Rather, the K_d may differ for structurally distinct regions of a crystal surface.

The observed partitioning differences between nonequivalent sectors are being used to constrain models of the atomic structure of the fluorite surface. Thus giving us a better understanding of the nature of the

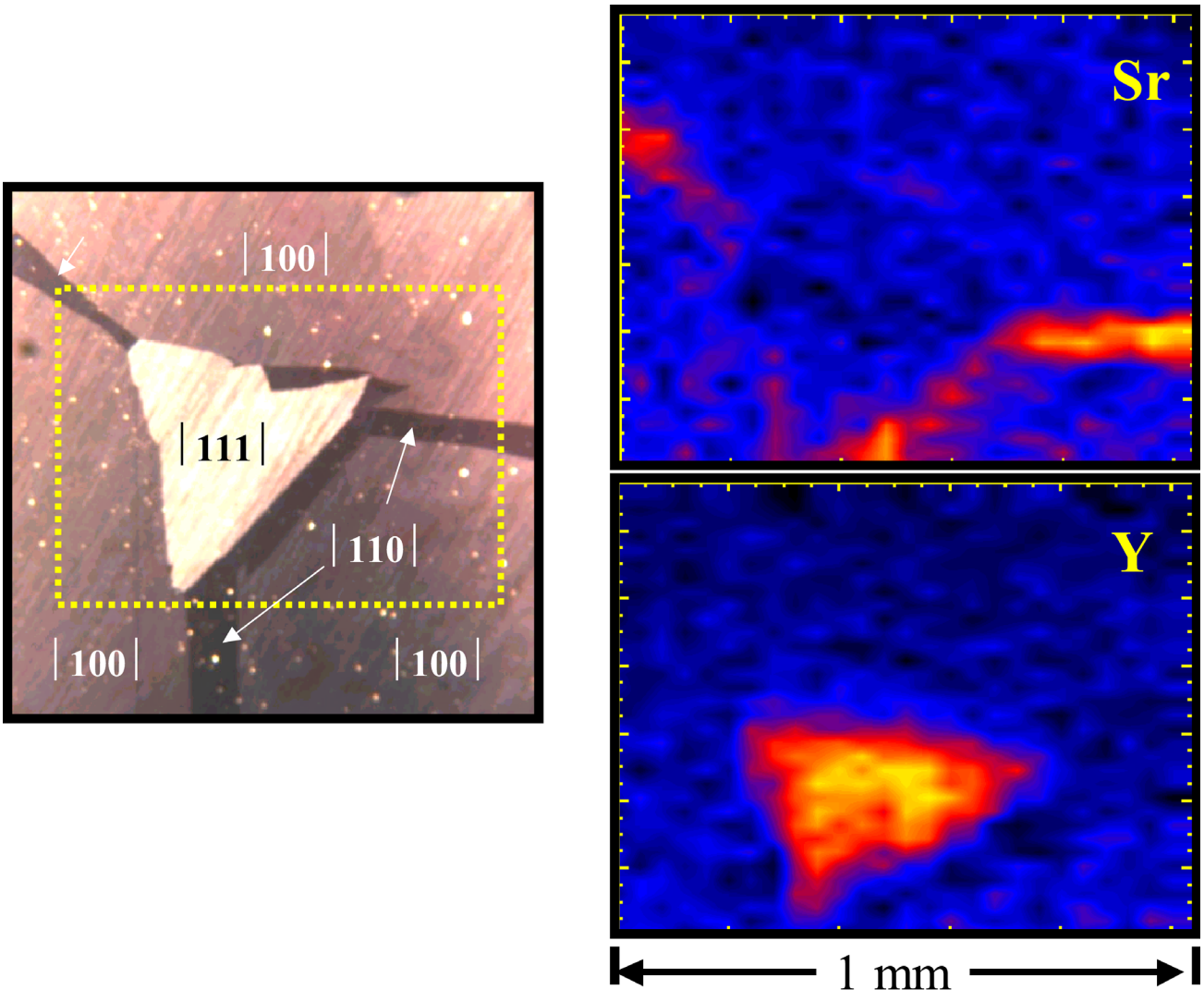

Figure 3. Sectoral zoning of Sr and Y in fluorite from Bingham, NM. The image on the left is an optical photomicrograph of a section cut through a single crystal of fluorite. Color zoning shows the internal morphology is comprised of |111|, |110| and |100| sectors. The top-right figure is a plot of the concentration of Sr (brighter colors represent higher concentration) for an area scan indicated by the yellow dashed line in the photomicrograph. The bottom-right figure is a plot of the concentration of Y (brighter colors represent higher concentration) for the same scan. Figure modified from Bosze and Rakovan (in Rev).

mineral-water interface and the mechanisms of differential incorporation during crystal growth.

Acknowledgments:

This work has been supported by NSF grant EAR-9814691.

References:

S. Bosze and J. Rakovan, " Surface Controlled Heterogeneous Incorporation of REE, Sr and Y in Fluorite". Annual Geological Society of America meeting, Abstracts with program. p. A-358, 1999.

S. Bosze and J. Rakovan, "Surface Controlled Non-Equilibrium Incorporation of the Rare Earth Elements in Fluorite from Long Lake, N.Y. and Bingham, N.M." In prep.

P.A. Northrup and R.J. Reeder, "Evidence for the importance of growth-surface structure to trace element incorporation in topaz" American Mineralogist, 79, 1167-1175, 1994.

J. Paquette and R.J. Reeder, "Relationship between surface structure growth mechanism, and trace element incorporation in calcite" Geochimica et Cosmochimica Acta, 59, 735-749, 1995.

J. Rakovan, M. Newville and S. Sutton (2001) "Wavelength dispersive XANES of heterovalent Eu in Llallagua apatite" American Mineralogist, in press.

J. Rakovan and R.J. Reeder, " Differential incorporation of trace elements and dissymmetrization in apatite: The role of surface structure during growth" American Mineralogist, 79, 892-903, 1994.

J. Rakovan and R.J. Reeder, "Intracrystalline rare earth element distributions in apatite: Surface structural influences on incorporation during growth" Geochimica et Cosmochimica Acta, 60, 4435-4445, 1996.

J. Rakovan, D.K. McDaniel, and R.J. Reeder "Use of surface-controlled REE sectoral zoning in apatite from Llallagua, Bolivia, to determine a single-crystal Sm-Nd age" Earth and Planetary Science Letters, 146, 329-336, 1997.

R.J. Reeder and J. Rakovan, "Surface structural controls on trace element incorporation during crystal growth" In *Growth, Dissolution and Pattern-formation in Geosystems*, B. Jamtveit and P. Meakin (eds.) p. 143-162. Kluwer Academic Publishers, 1999.

P.R. Richards and G.W. Robinson, "Mineralogy of the calcite-fluorite veins near Long Lake, New York" Mineralogical Record, 31, 413-422, 2000.

J.E. Taggart Jr., A. Rosenzweig, and E.E. Foord, "The Hansonburg District, Bingham, New Mexico" Mineralogical Record, 20, 31-46, 1989.